Journal of Pediatric Urology (2025) 21, 2–10

Expression of Wnt signaling proteins in rare congenital bladder disorders

Boyu Xie [a], Michael Millar [b], Callum Arthurs [a], Navroop Johal [c], Christopher Fry [d], Aamir Ahmed [a,e,*]

[a]Centre for Gene Therapy and Regenerative Medicine, Guy's Hospital, Great Maze Pond, King's College London, London SE1 9RT, UK

[b]Institute for Regeneration and Repair, University of Edinburgh, Edinburgh EH16 4UU, UK

[c]Department of Urology, Great Ormond Street Hospital for Children NHS Foundation Trust, London WC1N 3JH, UK

[d]School of Physiology, Pharmacology and Neuroscience, University of Bristol, Bristol BS8 1TD, UK

[e]Department of Cell and Developmental Biology, Rockefeller Building, University Street, University College London, London WC1E 6JJ, UK

* Correspondence to: Aamir Ahmed, Department of Cell and Developmental Biology, Rockefeller Building, University Street, University College London, London WC1E 6JJ, UK
aamir.ahmed@ucl.ac.uk
(A. Ahmed)

Keywords
Bladder exstrophy; Neurogenic bladder; Posterior urethral valves; Wnt signaling pathways; FRA1; Connexin 43

Received 30 May 2024
Revised 6 September 2024
Accepted 30 September 2024
Available online 5 October 2024

Summary

Introduction and aims
Congenital bladder anomalies are rare and are a leading cause of end stage renal failure in children. The Wnt signaling pathway, important during embryonic development, has been implicated in the pathogenesis of these conditions through regulation of gene expression, including essential transcription factors. We investigated the expression of four Wnt transcriptional targets, namely, Pygopus 1 (Pygo1), Connexin 43 (Cx43), FRA1 and TCF7L1 in three rare congenital bladder disorders: bladder exstrophy (BE), neurogenic bladder (NGB) and posterior urethral valves (PUV).

Methods
Bladder tissue samples were collected from patients at the Great Ormond Street Hospital for Sick Children, London, UK, with control (normally-functioning bladder, $N = 9$), BE ($N = 15$), NGB ($N = 6$) and PUV ($N = 5$). Histological analysis was performed using the van Gieson stain to differentiate smooth muscle (SM) and connective tissue (CT) compartments. An unbiased, automated, semi-quantitative immunofluorescence analysis was performed to measure the labelling intensity of four Wnt-related proteins in tissue from these four groups.

Results and discussion
There was a significant ($p < 0.05$) increase in the expression of Pygo1 in the smooth muscle of all anomalies examined and also in the connective tissue in PUV compared to control. Cx43 also showed overexpression in the smooth muscle across all conditions; however, there was a reduced expression in NGB and an increase in PUV in connective tissue. TCF7L1 showed a significant decrease in both tissue compartments for NGB, whereas FRA1 expression remained unchanged across all anomalies. We also measured colocalization of Wnt-related proteins. TCF7L1 exhibited increased colocalization with Pygo1 and FRA1 in exstrophy compared to control. These results suggest a complex dysregulation of the Wnt pathway in congenital bladder disorders.

Conclusion
Wnt signaling-related proteins show dysregulation in congenital bladder disorders compared to control tissue. Understanding these mechanisms should help towards non-invasive early diagnosis, drug target discovery and development of treatment strategies for these conditions.

https://doi.org/10.1016/j.jpurol.2024.09.029

Summary Table Summary of Wnt-related protein expression and colocalization in bladder exstrophy (BE), neurogenic bladder (NGB) and posterior urethral valves (PUV) disorder compared to normally-functioning control bladder. The table shows the levels of expression as significantly up (↑) down (↓) or no change (—) of Pygopus 1 (Pygo1), Connexin 43 (Cx43), FRA1 and TCF7L1 expression in smooth muscle and connective tissue compartments in BE, NGB and PUV relative to control bladder tissue samples. The table also shows colocalization of six protein pairs of Pygo1 and FRA1; Pygo1 and Cx43; Pygo1 and TCF7L1; FRA1 and Cx43; FRA1 and TCF7L1 and Cx43 and TCF7L1 in bladder disorders compared to control.

Protein Expression (Smooth muscle)				
	Pygo1	Cx43	FRA1	TCF7L1
BE	↑	↑	—	—
NGB	↑	↑	—	↓
PUV	↑	↑	—	—
Protein Expression (Connective tissue)				
BE	—	—	—	—
NGB	—	↓	—	↓
PUV	↑	↑	—	—

Colocalization						
	Pygo1/FRA1	Pygo1/Cx43	Pygo1/TCF7L1	FRA1/Cx43	FRA1/TCF7L1	Cx43/TCF7L1
Exstrophy	—	—	↑	—	↑	—
NGB	—	—	—	—	—	—
PUV	—	—	—	—	—	—

Introduction

The urinary bladder is primarily composed of smooth muscle (SM) and connective tissue (CT), the latter containing fibroblasts, interstitial cells, and various extracellular proteins including collagen, elastin, and fibronectin. It is thought that a number of congenital lower urinary tract abnormalities occur during 9—12 weeks post-fertilization affecting both the bladder and outflow tract [1]. We are particularly interested in three congenital bladder anomalies: (i) bladder exstrophy (BE) (ii) myelomeningocele-induced neurogenic bladder (NGB) and (iii) posterior urethral valves (PUV). BE is a pathology with bladder exposed outside of the abdominal wall, and with an incidence of approximately 1:30 000 [2]. NGB is hypoactive bladder with poor innervation and contractile function, and with an incidence 1:2000 [3]. PUV is the persistence of urethral valves in boys, leading to bladder outflow obstruction, with an incidence 1:4000—7500 [4]. There is little information on the underlying molecular mechanisms of these anomalies which although rare, can nonetheless have profound consequences for patients.

The wingless integration site (Wnt) signaling network is a highly conserved cell-to-cell communication pathway known to regulate embryonic and fetal development [5]. Wnt signal activation, in conjunction with various transcription factors, ultimately regulates gene transcription during cell proliferation and development in embryogenesis and proliferative diseases, such as cancers [6]. It is activated when secreted Wnt protein ligands interact with Frizzled receptors and lipoprotein receptor-related proteins (LRP) co-receptor to regulate cell membrane potential, activate intracellular calcium release, and regulate nuclear translocation of a transcription factor co-activator, β-catenin [6,7]. Not only does Wnt signaling play a critical role during development, its dysregulation is known to be involved in congenital disorders [8]. For example, dysregulation of Wnt in epiblast cells leads to linear cardiac tube malformations and causes congenital heart diseases [9]. Mutations or dysregulated expression of Wnt proteins and co-receptors in dorsal ectoderm is also linked with congenital upper limb abnormalities and bone/joint diseases [10].

Human genome-wide expression profiling has also revealed an association between Wnt3/6/7a/8b/10a/11/16 and FZD5, LRP1/10 genes and bladder exstrophy [11]. Wnt2 was also reported to regulate the size, proliferation, and contractile function of bladder smooth muscle cells [12]. We have previously assessed expression of some Wnt-related proteins (β-catenin, c-Myc, cyclin-D1, MMP-7) expression in BE [13], NGB [14] and PUV [4] with a focus on functionality and physiological changes of smooth muscle, without tissue type-specific analysis or cross-disease comparison of protein expression and colocalization. This study focusses upon the quantitation of Wnt-related protein expression in all three anomalies and extended our research in two distinct tissue types (smooth muscle and connective tissue) for a more comprehensive analysis.

Here we investigated the expression of four Wnt-related proteins Pygopus 1 (Pygo1), a Wnt transcription co-activator [15]; Connexin 43 (Cx43) [16], a protein proposed to translocate into the nucleus with β-catenin after Wnt signal activation; FRA1 [17] and TCF7L1 [18], Wnt targeted downstream transcription factors in BE, NGB and PUV tissue using an unbiased, semi-automated quantitative immunohistochemical approach. Our findings indicate a critical involvement of Wnt signaling dysregulation in the pathogenesis of these congenital anomalies.

Materials and methods

Ethical approval, patient information and tissue sample preparation

Ethical approval was granted by the UK Human Research Authority and the study was approved by the Great Ormond Street Hospital (GOSH) Research and Development department (ref: 04NU06). Ethical compliance was implemented through informed consent obtained from patients, guardians or Gillick-competent minors. Tissue samples from the anterior bladder wall were obtained from patients undergoing open surgeries such as bladder augmentation. Control samples were taken from patients with normal bladder function (for example urachal excision) at GOSH. Clinical information and patient ages corresponding to tissue samples is presented in Supplementary Table 1. Note that the median ages of the control and posterior urethral valves (PUV) groups were statistically smaller than the bladder exstrophy (BE) and neurogenic bladder groups (NGB).

The details of sample processing has been described elsewhere [19]. A total of 35 formalin-fixed paraffin-embedded (FFPE) tissue samples of control bladder and bladder abnormalities were obtained from the pathology archives of GOSH. Each tissue block was assigned a unique identifier number and anonymized to experimenters; the samples were only decoded once all the semi-automated, quantitative analysis was complete.

Sample size consideration

Despite conducting a preliminary sample size calculation [20], inherent rarity of the disorders under investigation, coupled with the limited availability of tissue samples, made the appropriate sample size impractical to achieve. An alternative approach was adopted, where one to three cores were extracted from stroma-rich areas of a single specimen, and therefore a greater number of cores were utilized ensuring sufficient analysis despite sample limitations [21].

Tissue array (TA) construction and sectioning

TAs were made using a MTA1 manual tissue arrayer (Beecher Instruments, Sun Prairie, WI, USA) as described earlier [22]. Briefly, tissue cores with 1 mm diameter and 3 mm depth were extracted from FFPE tissue samples. Two TA blocks, comprising 30 and 24 cores respectively, were constructed for van Gieson and antibody staining. TAs contained samples from: normally-functioning control bladders ($N = 9$, $n = 23$; N = number of patients, n = number of samples); BE ($N = 15$, $n = 15$); NGB ($N = 6$, $n = 6$); PUV ($N = 5$, $n = 10$). TAs were sectioned (6–8 μm) onto glass slides using a Thermo Scientific™ HM355S automatic microtome and used for subsequent histological and protein expression analysis. These processes are demonstrated in Supplementary Figure 1.

van Gieson staining, imaging and smooth muscle (SM) and connective tissue (CT) separation

van Gieson staining was used to distinguish SM from CT for reasons described in detail elsewhere [19]. Slides were scanned at 40× magnification using brightfield illumination on a NanoZoomer Digital Pathology scanner (Hamamatsu). Images were exported as .jpg files (11597 × 11597 pixel, 300 dpi). The van Gieson stained tissue cores were used to identify SM and CT areas for further protein expression analysis. An ImageJ algorithm that was developed in our lab was used to convert red (CT) and yellow (SM) van Gieson stained pixels to generate 8-bit grey scale images (Supplementary Figure 2) [19].

Multi-immunofluorescence labelling

The immunofluorescent labelling experiments were carried out double-blinded for both staining and imaging processes and decoded after the completion of all analyses. The Leica Biosystem Automated Bond RX™ IHC/ISH system was used to label multiple proteins following the previously published protocols [13]. To minimize experimental variability, all tissue array slides were stained concurrently. The following antibodies were used to detect the expression of Wnt-related proteins: Pygo1 (anti-Pygopus-1, 1:800, rabbit polyclonal, NGBP1-42665, Novus Biologicals), Cx43 (anti-connexin-43, 1:1000, rabbit polyclonal, C6219, Sigma—Aldrich), FRA1 (anti-FRA1, 1:2000, mouse monoclonal, ab117951, Abcam), and TCF7L1 (anti-human-TCF7L1, 1:200, mouse monoclonal, MAB61161, R&D Systems). Following primary antibody binding and detection with appropriate Horse Radish Peroxidase (HRP) secondary antibodies, Tyramide signal amplification (Akoya) [22,23] was used to for secondary labeling with coumarin, fluorescein isothiocyanate (FITC); Cy3 and Cy5, respectively.

Imaging and quantitative analysis

Multi-labeled TA slides were scanned at 20× magnification with a Zeiss AxioScan Z1 scanner (Cambridge, UK). Optimized parameters for imaging fluorophore-labelled four proteins were: Pygo1 (coumarin, 353/465 nm), Cx43 (FITC, 488/517 nm), FRA1 (Cy3, 577/603 nm) and TCF7L1 (Cy5, 633/671 nm — the colors rendered in figures are pseudo-colored and not spectral equivalents). All TA slides were imaged in a single session to minimize variations. Quantitative analysis of the intensity of each fluorophore was conducted using .czi image files.

The quantification of protein expression was based on the measurement of fluorescence intensity (AU) of each fluorophore, following methodologies detailed in previous study [19]. We analyzed the signal intensity for coumarin, FITC, Cy3, Cy5 within both SM and CT regions. To ensure accuracy, sister sections from the tissue array stained with van Gieson were aligned with the multi-labeled tissue cores to identify corresponding SM and CT regions (Supplementary Figure 2). Five regions of interest (ROIs), each with a 60 μm diameter circle (2829 μm^2), were marked in specific tissue type in each core using the 'draw circle' tool in Zen Blue 3.1 software. Protein expression was

quantified by measuring the signal intensity of each ROI for the four channels in Zen software. Intensity values of the four proteins in SM and CT were saved in an Excel file for further statistical analysis.

High magnification confocal microscopy and deconvolution for protein colocalization analysis

Protein colocalization can serve as a biomarker or indicate alterations in protein function in disease, in addition to changes in protein expression [20]. High-magnification images of multi-labeled slides were captured using a Leica SP8 confocal microscope (Leica, Milton Keynes, UK). The confocal settings for excitation/emission wavelengths were the same as described above, except for coumarin channel (405/429 nm). All tissue cores were imaged with a 63×1.4-NA oil objective lens, 6× optical zoom at 600 Hz in 1024 × 1024 pixel format. Approximately 26—30 Z-sections were obtained at sequential slice size of 0.17 μm. All settings including laser power, gain and offset were standardized at the start of the study and kept constant for imaging all tissue cores.

Subsequent to confocal imaging, deconvolution was performed using Huygens Professional software (SVI, The Netherlands) on confocal image files ('.lif' files). This converts image files into deconvolved '.H5' files for colocalization analysis. The global intersection coefficient (GIC) was then calculated, reflecting colocalization values between two channels. Therefore, four channels yield six pairs of combination: Pygo1/FRA1, Pygo1/Cx43, Pygo1/TCF7L1, FRA1/Cx43, FRA1/TCF7L1 and Cx43/TCF7L1. GIC values were exported to an Excel spreadsheet for further analysis.

Data analysis

All data from protein expression analysis are presented as median values with 25 % and 75 % interquartile ranges; non-normal distribution of datasets was determined using Kolmogorov—Smirnov tests. A Mann—Whitney U-test was used to compare protein expression in SM and CT between bladder disorder and control using MedCalc software (www.medcalc.org). The null hypothesis was rejected with a p-value <0.05. Boxplots demonstrating median and 25—75 % interquartile range were generated using Prism 9 software (GraphPad software, CA, USA).

Results

Quantitative expression of Pygo1, Cx43, FRA1 and TCF7L1 proteins in normal and diseased pediatric bladder

A representative multi-labeled fluorescence image illustrating the expression of Pygo1 (blue), Cx43 (green), FRA1 (orange), and TCF7L1 (purple) in control, BE, NGB and PUV tissue is shown in Fig. 1A—D. The pixel intensity (signal) for each fluorophore was quantified using an unbiased, semi-quantitative method [19] using Zen software for the SM and CT compartments by aligning sister sections from the

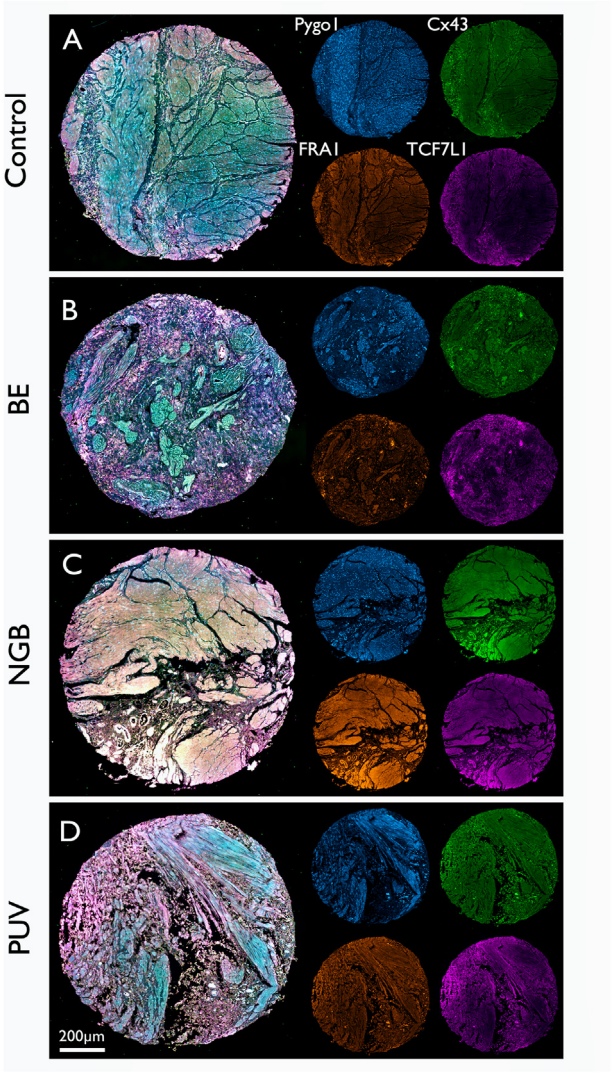

Fig. 1 Representative, composite, immunofluorescence images for multi-labelled tissue cores from control bladder (A), bladder exstrophy (BE, B), neurogenic bladder (NGB, C), and posterior urethral valves (PUV, D). The adjacent single-channel small cores on the right show individual labelling for Pygo1 (coumarin, blue), Cx43 (FITC3, green), FRA1 (Cy3, orange) and TCF7L1 (Cy5, purple). All images were scanned on an AxioScan Z1 (Zeiss) scanner at 20× magnification. Diameter of each core = 1 mm. (For interpretation of the references to color in this figure legend, the reader is referred to the Web version of this article).

van Gieson staining (see Supplementary Figure 2). Results are presented as boxplots with median values and 25 %, 75 % interquartile ranges.

The expression of four Wnt-related proteins was firstly analyzed in whole tissue cores without distinguishing between SM and CT components. As shown in Supplementary Figure 3, Pygo1 expression was significantly increased in PUV compared to controls. Cx43 expression was significantly decreased in BE and NGB but increased in PUV compared to normal bladder tissue. No significant differences were observed in FRA1 expression in any of the conditions tested. TCF7L1 expression was decreased only in

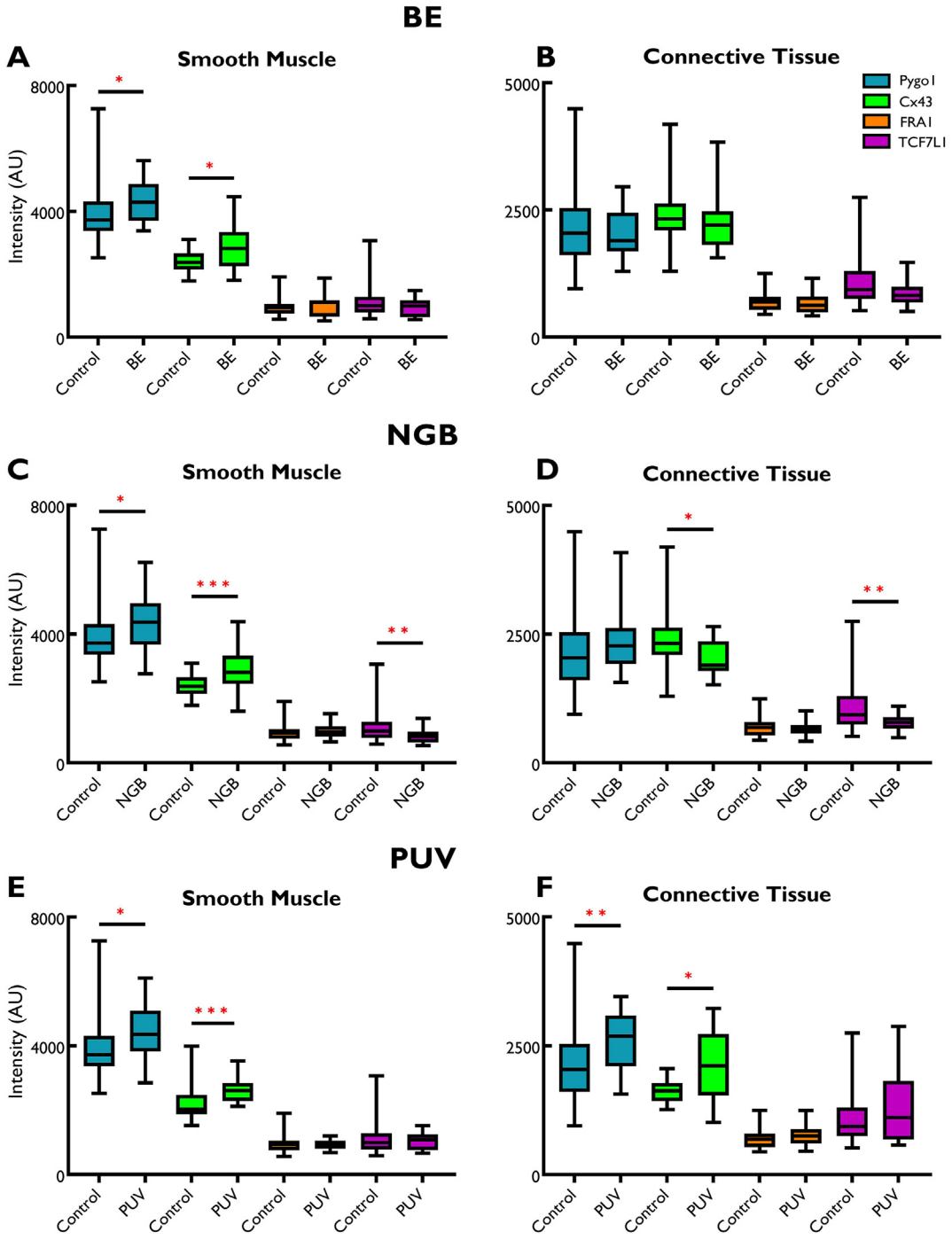

Fig. 2 Quantitative analysis of protein expression in bladder tissue. Boxplots show expression levels of Pygopus 1 (Pygo1), Connexin 43 (Cx43), FRA1 and TCF7L1 in smooth muscle and connective tissue in control (normal bladder) tissues versus those with bladder exstrophy (BE, A, B), neurogenic bladder (NGB, C, D), and posterior urethral valves (PUV, E, F). Protein expression is represented by fluorophore intensity (AU) measured from regions of interest (ROIs) using Zen Blue 3.1 software. Significance test (Mann—Whitney U-test) was carried out using GraphPad Prism 9 software (*$p \leq 0.05$; **$p \leq 0.01$; ***$p \leq 0.001$). (For interpretation of the references to color in this figure legend, the reader is referred to the Web version of this article).

NGB and not in the other two disorders when compared to controls.

However, the SM and CT components have different embryological origins and represent histologically and functionally distinct compartments of the bladder tissue. Therefore, the expression of proteins was also analyzed separately according to their tissue types. Fig. 2 shows quantitative analysis of the expression of four proteins in SM and CT in BE (Fig. 2A and B), NGB (Fig. 2C and D) and PUV (Fig. 2E and F) compared to control bladder tissue. The

expression of Pygo1 was significantly increased in SM of all three disorders compared to control; in CT, Pygo1 was only overexpressed in PUV compared to control bladder.

Cx43 also showed significantly increased levels in SM across all anomalies. However, there were significant differences in the expression of Cx43 in CT compartment: upregulated in PUV but downregulated in NGB compared to control. These results suggest a role for Pygo1 and Cx43 in the smooth muscle pathogenesis of the bladder. The upregulation of both proteins in the PUV smooth muscle may indicate the structural change of obstructed bladder.

TCF7L1 expression decreased in both smooth muscle and connective tissue of NGB, while FRA1 levels remained unchanged across all conditions and tissue types (Fig. 2). These results indicate that the suppression of Wnt-regulated transcription factor TCF7L1 in both SM and CT may suggest a distinct Wnt signaling mechanism in neurogenic bladder.

Interestingly, significant differences were observed in the quantitative expression of these proteins when analyzed as whole core versus separated SM and CT compartments (Supplementary Figure 3 and Fig. 2). For example, the consistent increase in Pygo1 and Cx43 expression in SM was not apparent in the whole core analysis. Additionally, the varying expression levels of these proteins between SM and CT were masked in the whole core

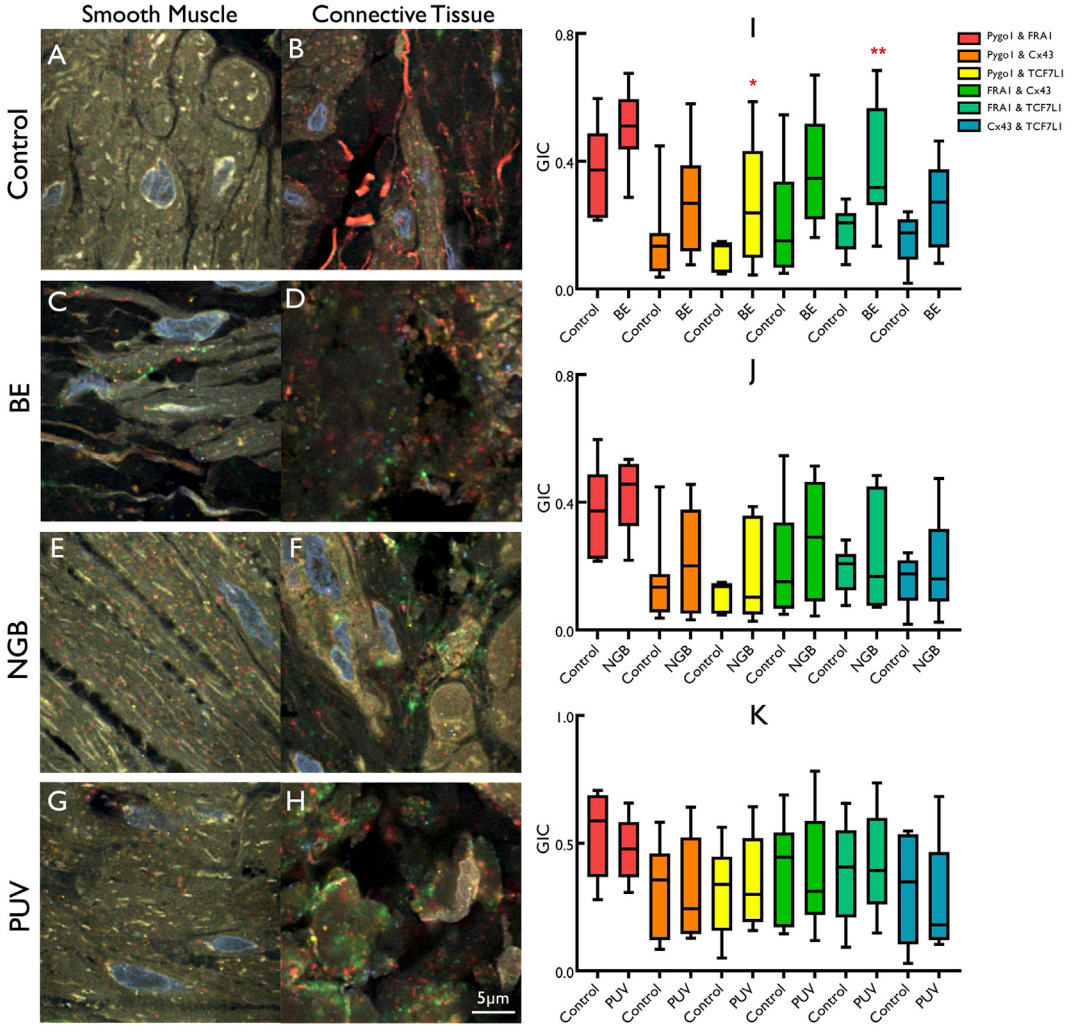

Fig. 3 Colocalization analysis in bladder tissue using confocal microscopy. Confocal images of four-antibody (Pygo1, Cx43, FRA1 and TCF7L1) labelled tissue in control bladder (A and B), bladder exstrophy (BE, C and D), neurogenic bladder (NGB, E and F) and posterior urethral valves bladder (PUV, G and H). The images differentiate regions of smooth muscle (A, C, E, G) and connective tissue (B, D, F, H). All images were captured with a Leica SP8 confocal microscope at 63× magnification and 6× optical zoom. Quantitative analysis of global intersection coefficient (GIC) value was performed for six protein pairs (Pygo1/FRA1; Pygo1/Cx43; Pygo1/TCF7L1; FRA1/Cx43; FRA1/TCF7L1 and Cx43/TCF7L1) comparing control tissue against- I) BE; J) NGB; K) PUV. Significance testing was carried out using Mann—Whitney U-tests using Prism 9 software (*$p \leq 0.05$; **$p \leq 0.01$; non-significant groups are not annotated). (For interpretation of the references to color in this figure legend, the reader is referred to the Web version of this article).

analysis. This result also emphasized the importance of tissue type segregation in the analysis of protein expression in bladder disorders.

Colocalization of proteins in normal and diseased bladder tissue

We routinely measure protein colocalization in addition to expression intensity measurements that can provide valuable information for diagnosis or prognostication [20]. In this study the GIC, a measure of colocalization, was compared for six paired protein combinations (Pygo1/FRA1, Pygo1/Cx43, Pygo1/TCF7L1, FRA1/Cx43, FRA1/TCF7L1 and Cx43/TCF7L1) in tissue from control samples and those from the three bladder disorders.

High-magnification (63x) confocal microscope images of the four fluorescence labels processed to measure GIC are presented in Fig. 3(A-H). The images are separated into SM (Fig. 3 A, C, E, G) and CT (Fig. 3 B, D, F, H) regions, providing examples of multi-labelled images for the four test proteins.

The GIC analysis revealed that Pygo1/TCF7L1 and FRA1/TCF7L1 exhibited increased colocalization in bladder exstrophy compared to control bladder ($p = 0.044$ and $p = 0.008$, respectively, Fig. 3 I). No other protein pair permutation showed any significant changes in GIC for BE, NGB, or PUV (Fig. 3J and K). A summary of all the quantitative analysis of protein expression and protein colocalization is presented in Table 1.

Discussion

Studies in numerous species of eukaryotes, such as *Drosophila melanogaster* (fruit fly), *Xenopus laevis* (frog), *Danio rerio* (zebrafish), and *Mus musculus* (mouse) have shown that Wnt is widely conserved and linked to body-axis development and malformations [5,6]. In *Homo sapiens* (human), Wnt signaling dysregulation is associated with a number of congenital disorders such as malformation of bones (*osteogenesis imperfecta*) [24], limbs (tetra-amelia syndrome) [25] and kidney [26], as well as omphalocele, which is sometimes accompanied by BE [27]. Indeed, the role of Wnts in body-axis determination and congenital anomalies including bladder anomalies has been previously suggested [6,13,14]. It is likely that bladder exstrophy and omphalocele, resulting from incomplete development of skin over the abdominal wall is associated with Wnt-regulated body axis formation during fetal development. Similar to exstrophy, myelomeningocele-induced neurogenic bladder is also represented as missing skin formation that results in incomplete closure of spinal cord [3]. Although neurogenic bladder is a secondary pathology, it is still a developmental defect and associated with body-axis formation. PUV, which results from an abnormal obstructing urethral membrane may be also caused by Wnt dysregulation.

We observed an increase of Pygo1, a Wnt-induced gene transcription co-activator, in smooth muscle tissue across all three disorders under investigation. Cx43, a protein proposed to translocate into the nucleus with β-catenin after Wnt signal activation [16], was also overexpressed in smooth muscle in all three disorders. This may indicate over-activation of Wnt signaling pathways. This hypothesis is supported by another study, which investigated the transcriptome of human bladder smooth muscle cells and found that the expression of the *WNT5A* gene was significantly increased in bladder exstrophy [28]. Hypertrophy is a common feature in bladder disorders investigated here and there is prior evidence linking hypertrophy with overexpression of Pygo 1 [29] and Cx43 in other tissue types [30]. Since Pygo1 overexpression-induced hypertrophy can also be reversed by β-catenin inhibition [29], this indicates the possibility of Wnt signaling over-activation in mesoderm

Table 1 Summary of Wnt-related protein expression and colocalization in bladder exstrophy (BE), neurogenic bladder (NGB) and posterior urethral valves (PUV) compared to normally-functioning control bladder. The table shows the levels of expression as significantly up (↑) down (↓) or no change (—) of Pygopus 1 (Pygo1), Connexin 43 (Cx43), FRA1 and TCF7L1 expression in smooth muscle and connective tissue compartments in BE, NGB and PUV relative to control bladder tissue samples. The table also shows colocalization of six protein pairs of Pygo1 and FRA1; Pygo1 and Cx43; Pygo1 and TCF7L1; FRA1 and Cx43; FRA1 and TCF7L1 and Cx43 and TCF7L1 in bladder disorders compared to control.

Protein Expression (smooth muscle)						
	Pygo1	Cx43	FRA1	TCF7L1		
Exstrophy	↑	↑	—	—		
NGB	↑	↑	—	↓		
PUV	↑	↑	—	—		
Protein Expression (connective tissue)						
Exstrophy	—	—	—	—		
NGB	—	↓	—	↓		
PUV	↑	↑	—	—		
Protein Colocalization						
	Pygo1/FRA1	Pygo1/Cx43	Pygo1/TCF7L1	FRA1/Cx43	FRA1/TCF7L1	Cx43/TCF7L1
Exstrophy	—	—	↑	—	↑	—
NGB	—	—	—	—	—	—
PUV	—	—	—	—	—	—

during embryonic development. Similarly, concordant expression of Cx43 and β-catenin has been reported in cardiac myocytes [31]; it is more likely that Cx43 overexpression also indicates overactive Wnt signaling in muscle tissue of these pediatric bladder anomalies. If this assessment is correct, it may suggest that overactive Wnt signaling, counterintuitively, may result in malfunction of abdominal wall closure.

Furthermore, TCF7L1, a transcription factor inhibited by Wnt signaling [32], was uniquely downregulated in neurogenic bladder in both SM and CT. This may indicate the suppression of TCF7L1 by Wnt activation in NGB. In addition to their protein expression, elevated colocalization of TCF7L1 with Pygo1 and FRA1 in bladder exstrophy could also indicate Wnt activation in this disorder. It should be noted that like all analytical measures, the methodology of measuring colocalization of proteins is not without its limitations. For example, the assessment distance between pixels from two different fluorophores does not imply protein—protein interaction, let alone altered protein function. Nevertheless, our observations emphasize the important role of Wnt in bladder formation and development, and its potential to be used as a therapeutic target. These analyses also provide a framework for further probing the role of Wnt signaling in congenital anomalies of the bladder.

It is likely that Wnt signaling may regulate bladder development via crosstalk with other signaling pathways, such as Wnt/planar cell polarity (PCP) and Wnt/TGF-β, emphasizing its multiple roles in bladder development and disorders. For instance, although it was argued that characterization of NGB is a spina bifida-induced neurological disorder, rather than a primary bladder disorder, studies have discovered Wnt/PCP signaling activation by loss of *Vangl1* and *Vangl2* genes in spina bifida [33]. This suggests an indirect involvement of Wnt activation in bladder conditions. Additionally, Wnt may regulate generation of congenital bladder disorders by altering the proportion of different tissue types. Our previous study demonstrate muscle tissue loss and accumulation of connective tissue in all three disorders compared to control [19]. Since Wnt activation promotes expression of connective tissue growth factor [34], it may explain why connective tissue is able to accumulate in bladder wall tissues.

Furthermore, Wnt/TGF-β signaling activation contributes to fibrosis, increases connective tissue build-up, inhibits degradation of extracellular matrix proteins, and thus reduces the smooth muscle/connective tissue ratio [19]. This line of evidence suggests a clear role for Wnt signaling in the physiological and functional alterations observed in bladder disorders, including contractile loss and decreased filling compliance.

Limitations

Any study that investigates changes to signaling pathways in albeit rare tissue samples from patients with extant lower urinary tract developmental anomalies must recognize that they may either be causal to the formation of such anomalies or secondary to pathophysiological functional changes that result from these anomalies. However, their value is to add focus to future studies of the importance, or otherwise, of particular signaling pathways in normal and abnormal lower urinary tract development and in larger studies to categorize potential secondary confounders.

Also, with regards to this investigation, the median ages of the patients donating tissue samples were greater in the BE and NB groups compared to the control and PUV groups (see Supplementary Table 1 for details). Future studies, using the same methodology, will add further data to these cohorts, but age-matching groups remains a slow process that depends on various clinical imperatives.

Conclusion

Our results highlight the complex network of Wnt signaling pathway and its distinct roles in bladder disorders during development. The dysregulation of key proteins Pygo1, Cx43, and TCF7L1, and altered colocalization patterns observed suggest that downstream gene transcription changes mediated by Wnt signaling may be fundamental to their pathology, offering new insight into understanding and potentially treating these conditions. Future research could focus on exploring the functional consequences of Wnt signaling alterations in bladder tissue. Additionally, expanding the study to include larger sample sizes and investigating other components of the Wnt pathway could provide a more comprehensive understanding of its role in bladder pathogenesis. Ideally, availability of animal models for congenital bladder disorders could shed light on the developmental dysregulation that result in these anomalies.

Ethical approval

Ethical approval was granted by the UK Human Research Authority and the study was approved by the Great Ormond Street Hospital (GOSH) Research and Development department (ref: 04NU06).

Conflict of interest

The authors have no relevant financial or non-financial interests to disclose. Part of the work presented here was submitted as a Master's thesis by the first author.

Acknowledgement

This work was supported by the Children's Research Fund, Liverpool, UK and supported by a generous donation to the Urological Foundation, UK from Mr and Mrs Miskin.

References

[1] Yiee J, Wilcox D. Abnormalities of the fetal bladder. Semin Fetal Neonatal Med 2008;13(3):164—70.
[2] Ben-Chaim J, Docimo SG, Jeffs RD, Gearhart JP. Bladder exstrophy from childhood into adult life. J R Soc Med 1996; 89(1):39P—46P.
[3] van Gool JD, Dik P, de Jong TP. Bladder-sphincter dysfunction in myelomeningocele. Eur J Pediatr 2001;160(7):414—20.

[4] Johal N, Cao K, Arthurs C, Millar M, Thrasivoulou C, Ahmed A, et al. Contractile function of detrusor smooth muscle from children with posterior urethral valves - the role of fibrosis. J Pediatr Urol 2021;17(1):100 e1—100 e10.
[5] van Amerongen R, Nusse R. Towards an integrated view of Wnt signaling in development. Development 2009;136(19): 3205—14.
[6] Li X, Ortiz MA, Kotula L. The physiological role of Wnt pathway in normal development and cancer. Exp Biol Med 2020;245(5): 411—26.
[7] Ashmore J, Olsen H, Sorensen N, Thrasivoulou C, Ahmed A. Wnts control membrane potential in mammalian cancer cells. J Physiol 2019;597(24):5899—914.
[8] Lu Y, Ren X, Wang Y, Han J. *Wnt signaling associated human diseases* novel techiniques. Arthritis & Bone Research 2018; 3(2):26—32.
[9] Mohamed IA, El-Badri N, Zaher A. Wnt Signaling: the double-edged sword diminishing the potential of stem cell therapy in congenital heart disease. Life Sci 2019;239:116937.
[10] Al-Qattan MM. WNT pathways and upper limb anomalies. J Hand Surg Eur 2011;36(1):9—22.
[11] Qi L, Chen K, Hur DJ, Yagnik G, Lakshmanan Y, Kotch LE, et al. Genome-wide expression profiling of urinary bladder implicates desmosomal and cytoskeletal dysregulation in the bladder exstrophy-epispadias complex. Int J Mol Med 2011; 27(6):755—65.
[12] Hashemi Gheinani A, Burkhard FC, Rehrauer H, Aquino Fournier C, Monastyrskaya K. MicroRNA MiR-199a-5p regulates smooth muscle cell proliferation and morphology by targeting WNT2 signaling pathway. J Biol Chem 2015;290(11):7067—86.
[13] Johal NS, Arthurs C, Cuckow P, Cao K, Wood DN, Ahmed A, et al. Functional, histological and molecular characteristics of human exstrophy detrusor. J Pediatr Urol 2019;15(2):154 e1—9.
[14] Johal N, Cao KX, Xie B, Millar M, Davda R, Ahmed A, et al. Contractile and structural properties of detrusor from children with neurogenic lower urinary tract dysfunction. Biology 2021;10(9).
[15] Kanwal B, Zen Y, Deheragoda M, Millar M, Thrasivoulou C, Rashid ST, et al. Comparative analysis of Wnt signaling-related proteins in normal, benign, malignant and metastasised human liver tumors. bioRxiv 2020. 2020.11.28.399865.
[16] Hou X, Khan MRA, Turmaine M, Thrasivoulou C, Becker DL, Ahmed A. Wnt signaling regulates cytosolic translocation of connexin 43. Am J Physiol Regul Integr Comp Physiol 2019; 317(2):R248—61.
[17] Arthurs C, Suarez-Bonnet A, Willis C, Xie B, Machulla N, Mair TS, et al. Equine penile squamous cell carcinoma: expression of biomarker proteins and EcPV2. Sci Rep 2020; 10(1):7863.
[18] Athanasouli P, Balli M, De Jaime-Soguero A, Boel A, Papanikolaou S, van der Veer BK, et al. The Wnt/TCF7L1 transcriptional repressor axis drives primitive endoderm formation by antagonizing naive and formative pluripotency. Nat Commun 2023;14(1):1210.
[19] Xie B, Johal N, Millar M, Thrasivoulou C, Kanai AJ, Ahmed A, et al. Quantification of the TGF- β/SMAD fibrosis pathway in bladder wall samples from children with congenital lower urinary tract anomalies. Continence 2023;5:100573.
[20] Arya M, Thrasivoulou C, Henrique R, Millar M, Hamblin R, Davda R, et al. Targets of Wnt/ss-catenin transcription in penile carcinoma. PLoS One 2015;10(4):e0124395.
[21] Hoos A, Cordon-Cardo C. Tissue microarray profiling of cancer specimens and cell lines: opportunities and limitations. Lab Invest 2001;81(10):1331—8.
[22] Xie B, Zuhair H, Henrique R, Millar M, Robson T, Thrasivoulou C, et al. Opposite changes in the expression of clathrin and caveolin-1 in normal and cancerous human prostate tissue: putative clathrin-mediated recycling of EGFR. Histochem Cell Biol 2023;159:489—500.
[23] Toth ZE, Mezey E. Simultaneous visualization of multiple antigens with tyramide signal amplification using antibodies from the same species. J Histochem Cytochem 2007;55(6): 545—54.
[24] Fahiminiya S, Majewski J, Mort J, Moffatt P, Glorieux FH, Rauch F. Mutations in WNT1 are a cause of osteogenesis imperfecta. J Med Genet 2013;50(5):345—8.
[25] Niemann S, Zhao C, Pascu F, Stahl U, Aulepp U, Niswander L, et al. Homozygous WNT3 mutation causes tetra-amelia in a large consanguineous family. Am J Hum Genet 2004;74(3): 558—63.
[26] Li Y, Pawlik B, Elcioglu N, Aglan M, Kayserili H, Yigit G, et al. LRP4 mutations alter Wnt/beta-catenin signaling and cause limb and kidney malformations in Cenani-Lenz syndrome. Am J Hum Genet 2010;86(5):696—706.
[27] Mallmann MR, Reutter H, Muller AM, Geipel A, Berg C, Gembruch U. Omphalocele-Exstrophy-imperforate anus-spinal defects complex: associated malformations in 12 new cases. Fetal Diagn Ther 2017;41(1):66—70.
[28] Michaud JE, Qiu H, DiCarlo HN, Gearhart JP. Inflammatory expression profiles in bladder exstrophy smooth muscle: normalization over time. Urology 2023;176:143—9.
[29] Lin L, Xu W, Li Y, Zhu P, Yuan W, Liu M, et al. Pygo1 regulates pathological cardiac hypertrophy via a beta-catenin-dependent mechanism. Am J Physiol Heart Circ Physiol 2021;320(4): H1634—45.
[30] Imamura M, Negoro H, Kanematsu A, Yamamoto S, Kimura Y, Nagane K, et al. Basic fibroblast growth factor causes urinary bladder overactivity through gap junction generation in the smooth muscle. Am J Physiol Ren Physiol 2009;297(1):F46—54.
[31] Ai Z, Fischer A, Spray DC, Brown AM, Fishman GI. Wnt-1 regulation of connexin43 in cardiac myocytes. J Clin Invest 2000;105(2):161—71.
[32] Shy Brian R, Wu C-I, Khramtsova Galina F, Zhang Jenny Y, Olopade Olufunmilayo I, Goss Kathleen H, et al. Regulation of Tcf7l1 DNA binding and protein stability as principal mechanisms of Wnt/β-catenin signaling. Cell Rep 2013;4(1):1—9.
[33] Mentink RA, Rella L, Radaszkiewicz TW, Gybel T, Betist MC, Bryja V, et al. The planar cell polarity protein VANG-1/Vangl negatively regulates Wnt/β-catenin signaling through a Dvl dependent mechanism. PLoS Genet 2018;14(12):e1007840.
[34] Luo Q, Kang Q, Si W, Jiang W, Park JK, Peng Y, et al. Connective tissue growth factor (CTGF) is regulated by Wnt and bone morphogenetic proteins signaling in osteoblast differentiation of mesenchymal stem cells. J Biol Chem 2004; 279(53):55958—68.

Appendix A. Supplementary data

Supplementary data to this article can be found online at https://doi.org/10.1016/j.jpurol.2024.09.029.